Effects of Thermally Induced Distress on Adhesively Bonded Piezoelectric Wafer Active Sensors and Implications on Damage Detection and Localization

Jesus Eiras, Ludovic Gavérina, Loïc Mastromatteo, Jean-Michel Roche

Effects of Thermally Induced Distress on Adhesively Bonded Piezoelectric Wafer Active Sensors and Implications on Damage Detection and Localization

JESUS N. EIRAS, L. GAVÉRINA, L. MASTROMATTEO
and J. M. ROCHE

ABSTRACT

Structural Health Monitoring (SHM) systems enable informing on structural health on a continuous time basis, resulting in optimized maintenance and reduced risk of failure. However, airborne equipment is commonly subjected to harsh environments including extremely high and low temperatures, transient loads, humidity, or radiation. As a result, the sensing function gradually degrades, ultimately impairing the performance of the SHM system to detect and localize damage. In this study, we analyze through two numerical experiments the effects that degrading bonding PWAS interface may produce on electromechanical impedance measurements and guided wave propagation testing. The first experiment investigates the effects of degraded adhesive bonding on electromechanical impedance and guided wave emission using a Finite Element Model (FEM). The results demonstrate that PWAS debonding modifies the electromechanical response, producing considerable distortion on the generated and received wave fields. The alteration of the bonding layer affects the wave tuning curve, resulting in non-uniform wave amplitudes across the plate. The second experiment focuses on the impact of PZT bonding degradation on damage localization. A circular sensor layout with multiple PWAS was considered. The FEM is solved for both intact and damaged plates, as well as for partially bonded PWAS. Tomographic imaging algorithms, including RAPID and Delay-and-Sum (DAS) were used. In summary, this study emphasizes the significance of understanding the effects of degraded bonding in PWAS for a more accurate assessment of aeronautical structures.

INTRODUCTION

The benefits of adopting Structural Health Monitoring (SHM) in the aeronautical industry are widely recognized [1]. However, aeronautic structures are exposed to harsh environments characterized by extreme temperatures, dynamic and transient loads, humidity, and UV radiation. These environmental factors can lead to the deterioration of airborne equipment, thus, gradually impairing the sensing function of SHM systems and compromising their performance. Among the different sensing technologies available, Piezoelectric Wafer Actuator Sensors (PWAS) are attractive for SHM applications because of their lightweight construction, low-power energy consumption, and ability to be mounted on structures with inconsequential impact on their mechanical properties. Besides, well-documented SHM interrogation techniques, including electrical impedance, guided wave testing, or acoustic emission can rely on PWAS [2]. Despite the multiple advantages that PWAS present, they are not exempt from durability issues. These include bonding degradation, physical sensor cracking, soldering breakage, and piezoelectric property waning. The reliability analysis of SHM systems is therefore paramount for addressing the durability concerns of PWAS.

Jesús N. Eiras, Ludovic Gavérina, Loïc Mastromatteo, Jean-Michel Roche, DMAS, ONERA, Université Paris-Saclay, F-92322 Châtillon, France.

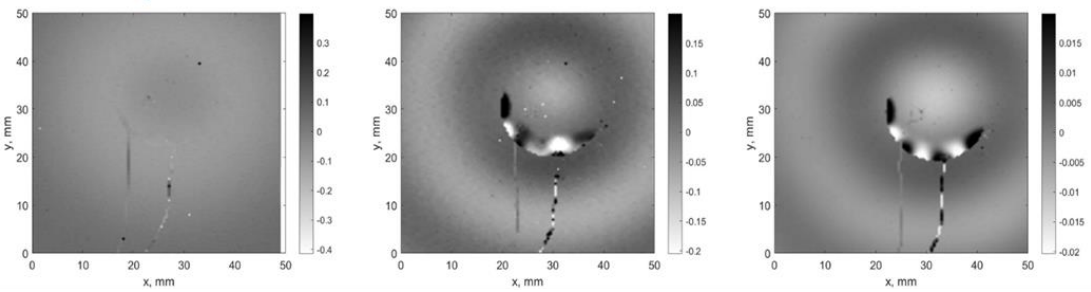

Figure 1. Evolution of the out-of-plane velocity response at 25kHz measured on a PWAS after 0, 350, and 525 cycles bonded PZT to the aluminum plate. Adapted from [7].

Thermal cycling under representative temperature extremes is often used to accelerate PWAS disbonding and provide insight into their long-term performance. Electromechanical impedance (EMI) measurements and laser vibrometer scanning are the preferred testing solutions in the literature to apprehend the effects of degraded bonding in PWAS [3], [4]. Both techniques provide valuable insights into the performance of embedded [5] and surface mounted [6] sensors. Figure 1 shows a representative example of the vibration response at 25kHz of a PWAS bonded to an aluminum plate; results for the healthy reference and after 350 and 525 cycles of thermal cycling between -55°C and 85°C are shown [7]. The results shown in Figure 1 exemplify reveal that PWAS sensors exhibit important amplitudes as it starts to debond. As a result, such modification of boundary conditions is manifested as an alteration on the EMI spectra. These experimental results are qualitatively similar to those reported in previous studies [4], [8], [9]. Besides, further experimental evidence obtained elsewhere through ultrasonic pitch-catch measurements [3], [6], [10], [11], include meaningful decrease in the amplitude of the transmitted and received signals (or increase, depending on the driven frequency), and linear phase shifts. While these contentions only prove that PWAS are still capable functioning, the generated waves in the inspected structure may not be useful to detect or localize damage (false negative) or else, may generate false indication of damage (false positive). In this study, we analyze through two numerical experiments the effects that degrading bonding PWAS interface may produce on electromechanical impedance measurements (self-diagnose method) and guided wave testing.

NUMERICAL EXPERIMENTS

Numerical Experiment 1: Effect of degraded adhesive bonding on electromechanical impedance and guided wave emission

The effects of PWAS adhesion loss on its electrical impedance were analyzed through a Finite Element Model (FEM). Figure 2 shows a schematic representation of the FEM model. The model consists of a circular elastic plate (thickness of 2.4mm) flanked by reflectionless boundary conditions and one piezoelectric disc (radius 10mm and 0.2mm thick) attached to one of the plate surfaces. Thin elastic layer elements were used to model the adhesive attachment between the PWAS and the aluminum plate. The normal and tangential stiffness (k_n and k_t) of such interface elements are obtained from

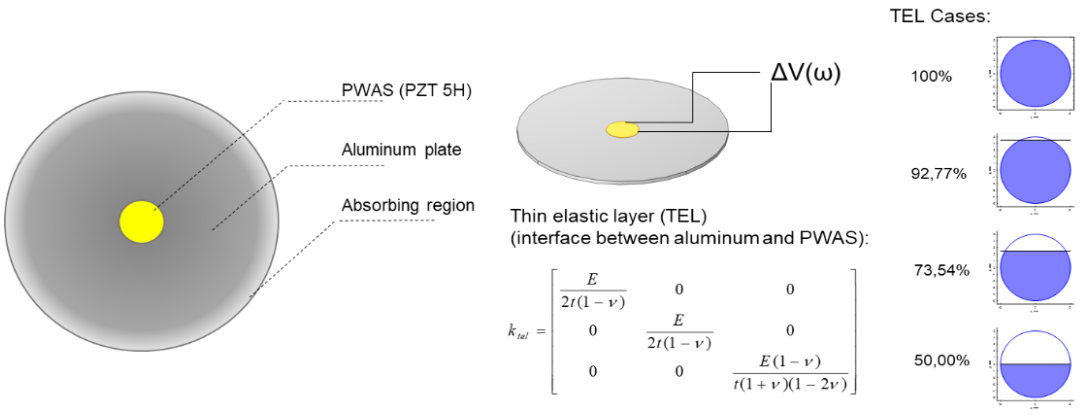

Figure 2. Schematic representation of the FEM for EMI and wave propagation. Different boundary conditions were set in between the PWAS and the aluminum plate to model different debonded extents.

the adhesive thickness (t) and elastic properties (Young's modulus (E_{tel}) and Poisson's ratio (v_{tel})) as

$$k_t = \frac{E}{2t(1-\nu)}, \tag{1}$$

$$k_n = \frac{E(1-\nu)}{t(1+\nu)(1-2\nu)} \tag{2}$$

Herein, Young's modulus and Poisson's ratio of the adhesive layer were set to 1GPa and 0.30. The density and thickness were set to 1100 kg/m^3 and 100 µm. To investigate the effect of a degraded interface a parametric study was conducted by incrementally reducing the bonded area as shown in Figure 2. The unbonded zone was defined by setting stiffness and mass to zero. The harmonic response of the system was evaluated in the frequency domain from 10kHz to 350kHz at frequency steps of 1kHz, for all the considered scenarios.

Figure 3a shows the modulus of the electrical admittance spectra ($|Y(\omega)|$) obtained for a perfect bond and increasing. The results show that for the perfect bond (100%), the modulus of the admittance increases monotonically with frequency and then exhibits a first resonant mode at ~325kHz. Contrariwise, the extent of the debonding modifies the electromechanical response by promoting new resonant modes. Several Damage Indices have been proposed to detect deviations from a healthy baseline, such as the Root Mean Squared Error (RMSE), the Correlation Coefficient (CC), or the slope of the susceptance (imaginary admittance) spectra [3]. A discussion of the sensitivity of the different damage index to detect different PWAS failure modes can be found in [9]. Remarkably, the lowest debonded area studied herein (92.77%) produces very little alteration of the EMI spectra.

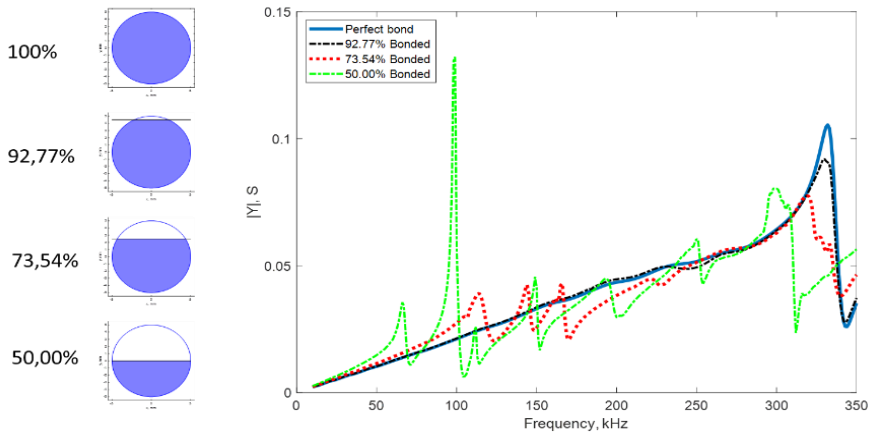

Figure 2. Modulus of the admittance spectra obtained for perfectly and partially bonded PWAS.

Figure 3 shows representative out-of-plane displacement fields generated at selected frequencies (25kHz, 100kHz, and 200kHz) for a perfect bond (100%) and one deteriorated bond (73.54%). The results reveal that the omnidirectional wave field expectation for a perfect bond was altered, producing varying wave amplitudes throughout the plate. Interestingly, in some instances resulted even in enhanced amplitude at some particular frequencies (see for instance the results obtained at 100kHz). This outcome result is a direct consequence of wave tuning curve change. Figure 4 compares the wave tuning curves obtained from FEM for perfect and partially (73.54%) bonded PWAS. Theoretical wave tuning curve formulae for ideally bonded PWAS can be found in [12], [13]. Herein, wave tuning local minima for the antisymmetric A_o mode were found at ~100kHz and ~250kHz,. The modification of the bond geometry lead to considerably distortion of the wave tuning curve shifting and producing local minima and maxima for symmetric and antisymmetric modes across the plate. These results were also observed for lesser-debonded layers considered herein (, these results are not shown for the sake of brevity).

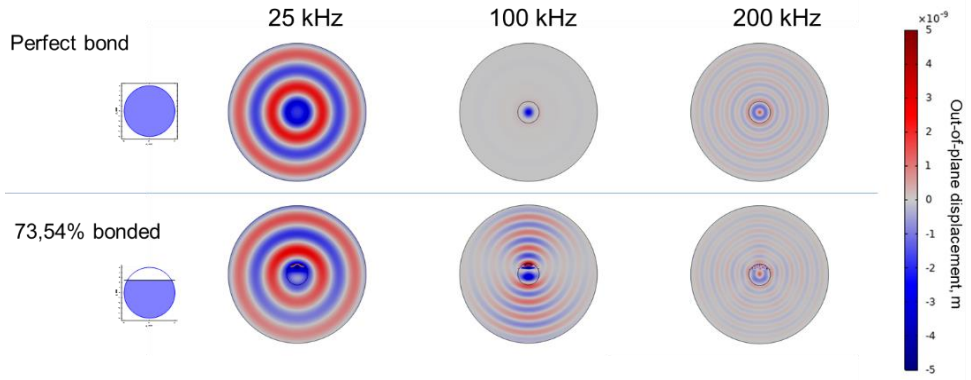

Figure 3. Out-of-plane displacement field at 25kHz, 100kHz, and 200kHz obtained for a perfectly bonded PWAS and a partially bonded (73.54%) PWAS.

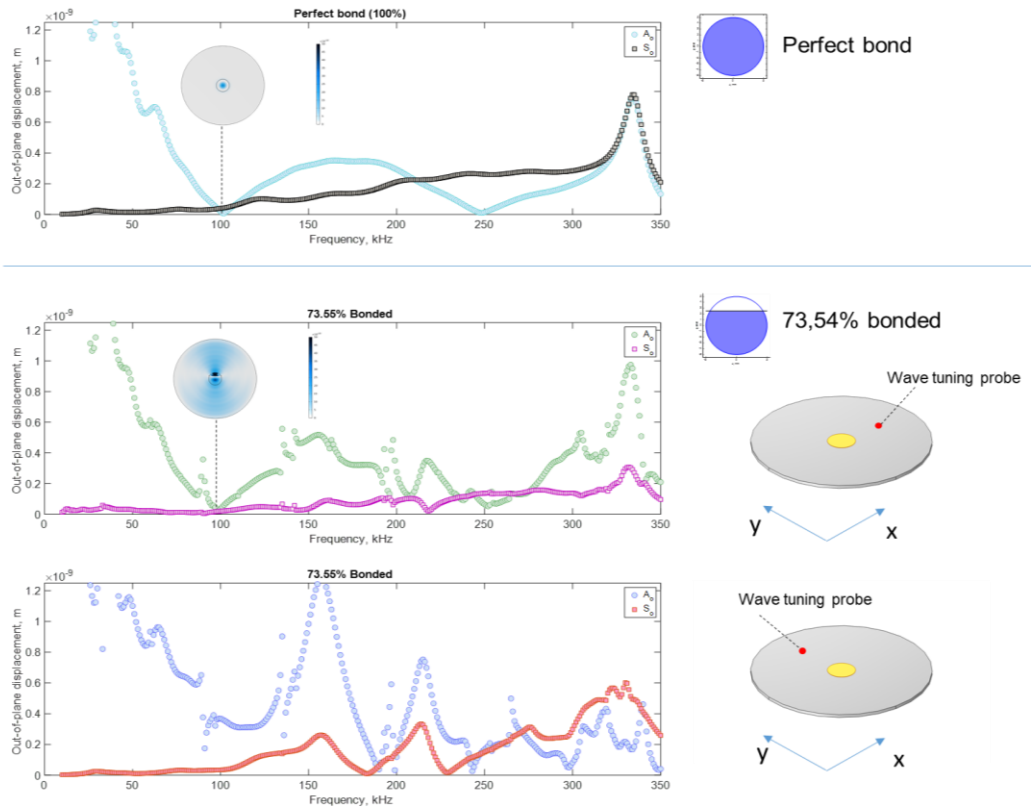

Figure 4. Wave tuning curves obtained for a perfectly bonded PWAS and a partially bonded (73.54%) PWAS.

Numerical experiment 2: Impact of PZT bonding degradation on damage localization

The second numerical experiment consists of a circular sensor layout of N= 5 PWAS (diameter 10mm, thickness 0.2mm, and type PZT 5H) attached to an aluminum plate (500x500x2.4 mm) with Young's modulus of 65GPa, Poisson's ratio of 0.33, and density of 2750kg/m^3. The spatial and temporal discretization were determined based on the minimum wavelength and in accordance with the Courant-Friedrichs-Levy condition.—$\Delta t = \Delta x/(c_{\max}\sqrt{3})$, wherein $\Delta x = \lambda_{\min}/10$—. Figure 5 schematically describes the FEM. A voltage potential consisting of an amplitude-modulated 3-cycle sine burst with a center frequency of 150kHz was applied onto one of the piezoelectric domains, while the remaining ones acted as receivers. The mechanical wave generated by the emitter *i* results in electrical charge (*Q*) because of the direct piezoelectric in the remaining *N-1* receivers. The process is recursively repeated for each of the sensors following a round-robin approach. The FEM was solved for the intact plate to obtain a reference dataset of baseline waveforms representative of the healthy state. Then, a damaged plate was considered by reducing mass and Young modulus by 50% on a local spot (defect size of 15mm) of the plate. To investigate the effects of a degraded PWAS bond on damage detection and localization, the overall process was solved also for partially bonded PWAS. In this later case, all the sensors had equal bonded area (89.96%) but different orientations (see Figure 5).

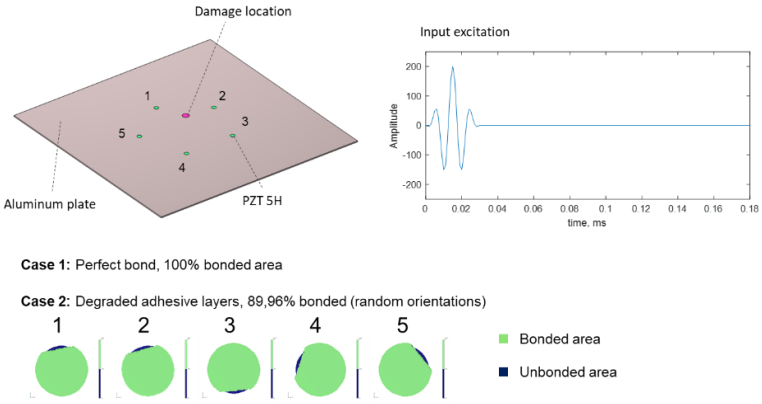

Figure 5. Representative residual signals obtained for damaged.

Two well-known algorithms, RAPID and Delay-and-Sum (DAS) are commonly used on sparse array sensor data to localize damage in plate-like structures. First, in the RAPID algorithm —Reconstruction Algorithm for Probabilistic Inspection of Damage [14]—, the tomographic image is obtained by weighting a particular signal feature ($A_{RAPID,k}$) by a spatial weighting function $w_{i,j}(x,y)$ and summing up the total contribution of the $N{\cdot}(N\text{-}1)$ paths as

$$I_{RAPID}(x,y) = \sum_{k=1}^{N(\cdot N-1)} w_{i,j}(x,y) \cdot A_{RAPID,k} \tag{3}$$

wherein the weighting function ($w_{i,j}(x,y)$) is defined as

$$w_{i,j}(x,y) = \begin{cases} \dfrac{\beta - d_{i,j}(x,y)/L_{i,j}}{\beta - 1}, & for\ \beta > \dfrac{d_{i,j}(x,y)}{L_{i,j}} \\ 0, & for\ \beta \le \dfrac{d_{i,j}(x,y)}{L_{i,j}} \end{cases} \tag{4}$$

wherein, β is a scaling parameter (herein set to 1.8) and ($d_{ij}(x,y)$) is the sum of the round trip distance from the emitter i to receiver j passing through every pixel (x,y) coordinates, and $L_{i,j}$ is the path length. Herein, the signal feature $A_{RAPID,k}$ was defined as the sum of absolute differences between reference and damage states.

The second algorithm is the Delay and Sum (DAS) algorithm. Likewise, by summing up $N{\cdot}(N\text{-}1)$ signal features leads to the resulting DAS tomographic image

$$I_{DAS}(x,y) = \sum_{k=1}^{N\cdot(N-1)} A_{DAS,k}(x,y) \tag{5}$$

wherein the $A_{DAS,k}(x,y)$ is the amplitude residual kth waveform ($r_k(t)$), obtained at the time corresponding to the roundtrip distance from emitter i to receiver j passing through the pixel (x,y) as

$$A_{DAS,k}(x,y) = \left| \mathrm{H}\left(r_k\left(\frac{d_{ij}(x,y)}{c_g} + t_{off} \right) \right) \right| \tag{6}$$

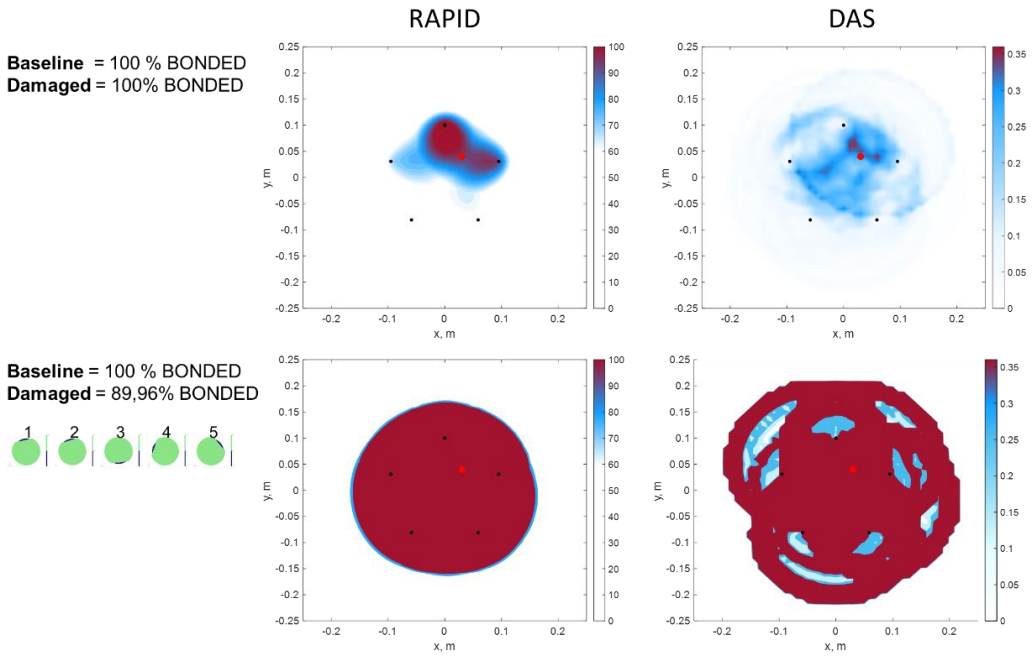

Figure 6. Tomographic images for RAPID and DAS algorithms for perfectly bonded PWAS, and comparison with PWAS bond degradation (baseline obtained with perfectly bonded PWAS and damaged with partially bonded PWAS)

wherein H(·) denotes the Hilbert transform. Only the antisymmetric A_o mode was used herein, for which its group velocity was found to be 2623 m/s, and t_{off} was set to half duration of the input signal. Figure 6 compares the obtained tomographic images using RAPID and DAS algorithms. The results clearly demonstrate that a small reduction in the bonding surface (only ~10% of reduction) significantly hampers the localization of damage.

DISCUSSION, CONCLUSION AND PERSPECTIVES

The present study emphasizes the challenges posed by harsh environmental conditions that can gradually deteriorate Piezoelectric Wafer Actuator Sensors (PWAS) bonding, which may ultimately lead to false indication of damage or compromising the detection and localization of damage. Two numerical experiments were presented to investigate these effects. The first experiment focused on the effects of degraded adhesive bonding on electromechanical impedance and guided wave fields using a Finite Element Model (FEM). The results confirm that debonding of PWAS significantly modifies its electromechanical response, which confirms the potential of using Electromechanical Impedance (EMI) as a nondestructive inspection technique for bonded PWAS. However, the results also highlight that even slight alterations of the adhesive layer may produce little modification in the EMI spectra, yet produce considerable distortion of the generated wave field. The latter was substantiated by evaluating the PWAS wave tuning curves. Additionally, a sensor layout consisting of five PWAS bonded to a metallic plate was modeled. The objective of this numeric experiment aimed at evaluate the effects of deteriorated PWAS bond layer on damage

localization. The Delay-and-Sum and RAPID algorithms were used to this purpose. The results demonstrated that little modifications of the sensor bonding layers impaired the accurate localization of damage.

REFERENCES

1. Staszewski, W. J., Boller, C., & Tomlinson, G. R. (2003). Health Monitoring of Aerospace Structures: Smart Sensor Technologies and Signal Processing. John Wiley & Sons, Ltd.
2. Giurgiutiu, V. (2007). Structural Health Monitoring: With Piezoelectric Wafer Active Sensors. Elsevier.
3. Park, G., Farrar, C. R., Scalea, F. L. di, & Coccia, S. (2006). Performance assessment and validation of piezoelectric active-sensors in structural health monitoring. Smart Materials and Structures, 15(6), 1673–1683. https://doi.org/10.1088/0964-1726/15/6/020
4. Mueller, I., & Fritzen, C.-P. (2017). Inspection of Piezoceramic Transducers Used for Structural Health Monitoring. Materials, 10(1), 71. https://doi.org/10.3390/ma10010071
5. Kergosien, N., Gavérina, L., Ribay, G., Saffar, F., Beauchêne, P., Mesnil, O., & Bareille, O. (2023). Lead Zirconate Titanate Transducers Embedded in Composite Laminates: The Influence of the Integration Method on Ultrasound Transduction. Materials, 16(8), Article 8. https://doi.org/10.3390/ma16083057
6. Mastromatteo, L., Gaverina, L., Lavelle, F., Roche, J.-M., & Irisarri, F.-X. (2023). Thermal Cycling Durability of Bonded PZT Transducers Used for the SHM of Reusable Launch Vehicles. In P. Rizzo & A. Milazzo (Eds.), European Workshop on Structural Health Monitoring (pp. 727–736). Springer International Publishing. https://doi.org/10.1007/978-3-031-07258-1_73
7. Gavérina, L., Roche, J.-M., Beauchêne, P., & Passilly, F. (2021). Study of the effects of thermal stress on piezoelectric sensors for the Structural Health Monitoring. International Workshop on Structural Health Monitoring. https://doi.org/10.12783/shm2021/36353
8. Mueller, I., Shpak, A., Golub, M. V., & Fritzen, C.-P. (2016). Effects of Debonding of PWAS on the Wave Propagation and the Electro-Mechanical Impedance Spectrum. European Workshop On Structural Health Monitoring (EWSHM 2016), 5-8 July 2016, Spain, Bilbao
9. Mueller, I., & Fritzen, C.-P. (2018). Failure Assessment of Piezoelectric Actuators and Sensors for Increased Reliability of SHM Systems. In M. A. Wahab, Y. L. Zhou, & N. M. M. Maia (Eds.), Structural Health Monitoring from Sensing to Processing. InTech. https://doi.org/10.5772/intechopen.77298
10. Mulligan, K., Quaegebeur, N., Ostiguy, P.-C., Masson, P., & Létourneau, S. (2012). Comparison of metrics to monitor and compensate for piezoceramic debonding in structural health monitoring. Structural Health Monitoring, 12, 153–168. https://doi.org/10.1177/1475921712467490
11. Lanzara, G., Yoon, Y., Kim, Y., & Chang, F.-K. (2009). Influence of Interface Degradation on the Performance of Piezoelectric Actuators. Journal of Intelligent Material Systems and Structures, 20(14), 1699–1710. https://doi.org/10.1177/1045389X09341198
12. Giurgiutiu, V. (2005). Tuned Lamb Wave Excitation and Detection with Piezoelectric Wafer Active Sensors for Structural Health Monitoring. Journal of Intelligent Material Systems and Structures, 16(4), 291–305. https://doi.org/10.1177/1045389X05050106
13. Raghavan, A., & Cesnik, C. E. S. (2004). Modeling of piezoelectric-based Lamb wave generation and sensing for structural health monitoring (S.-C. Liu, Ed.; p. 419).
14. Hay, T. R., Royer, R. L., Gao, H., Zhao, X., & Rose, J. L. (2006). A comparison of embedded sensor Lamb wave ultrasonic tomography approaches for material loss detection. Smart Materials and Structures, 15(4), 946–951. https://doi.org/10.1088/0964-1726/15/4/007.